IJR International Journal of Railway
Vol. 1, No. 3 / September 2008, pp. 99-105

The Korean Society for Railway

Computer Simulation of a Train Exiting a Tunnel through a Varying Crosswind

S. Krajnović†

Abstract

Flow around an ICE2 high-speed train exiting a tunnel under the influence of a wind gust has been studied using numerical technique called detached eddy simulation. A wind gust boundary condition was derived to approximate previous experimental observations. The body of the train includes most important details including bogies, plugs, inter-car gaps and rotating wheels on the rail. The maximal yawing and rolling moments which possibly can cause a derailment or overturning were found to occur when approximately one third and one half of the train, respectively, has left the tunnel. These are explained by development of a strong vortex trailing along the upper leeward edge of the train. All aerodynamic forces and moments were monitored during the simulation and the underlying flow structures and mechanisms are explained.

Keywords : *Crosswind stability, Wind gust, High-speed train, Detached eddy simulation*

1. Introduction

Most investigations of crosswind effects on trains have in past been that of steady cross winds. The simple explanation for such a situation is found in difficulty of performing numerical and experimental studies of trains in gusty conditions.

Howell and Everitt [1] and Howell [2] studied experimentally forces and moments on a simplified high speed maglev train passing through a cross wind. The gusty condition in their study was obtained by propelling a train model through a stationary cross wind. They observed that the peak yaw moment was about 20% larger compared to the steady crosswind situation.

Other examples of studies of effects of wind gusts on ground vehicles are for road vehicles such as that by Kobayashi and Yamada [3] who experimentally studied simple one-box vehicles entering a region of crosswind. Their objective was to study the yawing moment acting on a vehicle which was much shorter than the width of the crosswind region. Unfortunately this is not applicable to trains which are normally rather long.

An interesting study is that by Ryan and Dominy [4] who studied a generic vehicle in a specially constructed wind tunnel arrangement which simulated a wind gust of finite length. The target of their study was the impact of the wind gust on the wake. The shape of the typical gust from their study was used in the present paper to approximate the mathematical model of the wind gust used in the simulation.

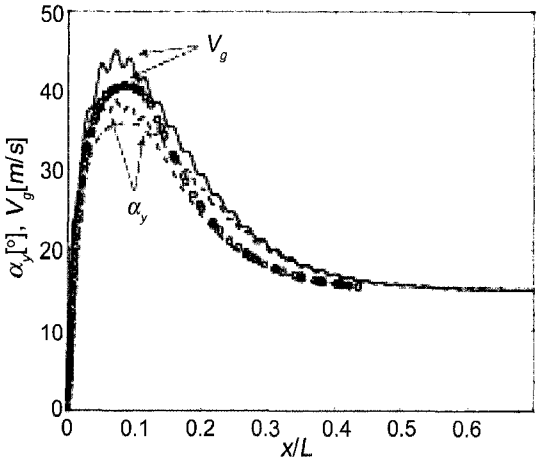

Fig. 1. Model of the Wind Gust. Lateral Velocity Component: V_g Applied on the Boundaries of the Domain (Solid Line); that Reaches the Train (Circles). Yaw Angle α_y between the Streamwise Velocity and the V_g: Applied on the Boundaries of the Domain (Dashed Line); that Reaches the Train (Dashed-dotted Line). L is the Length of the Train

† Chalmers University of Technology, Department of Applied Mechanics SE 412 96 Gothenburg, Sweden

There are two typical scenarios where trains are affected by wind gusts: a train is exiting a tunnel under the influence of a wind gust and a train travelling on an embankment is influenced by a wind gust. In the present paper we present the results of a numerical investigation of the former scenario where the moving train is exiting the tunnel and passing through a crosswind profile constant in time which has the shape presented in Fig. 1. The idea is that the train is passing through a region of finite length with varying crosswind velocity and ends in a constant crosswind. During this passage the train is influenced by varying crosswind magnitude and thereby a varying yaw angle of the crosswind.

2. Boundary Conditions and the Train Model

The computational domain for the train leaving the tunnel is shown in Fig. 2a. The simulation is first run with only one inlet and the constant velocity profile at the inlet of 56 [m/s]. This velocity corresponds to a train moving at speed of 200 [km/h] which is maximal speed of X2000 train operating in Sweden. When the flow has developed,

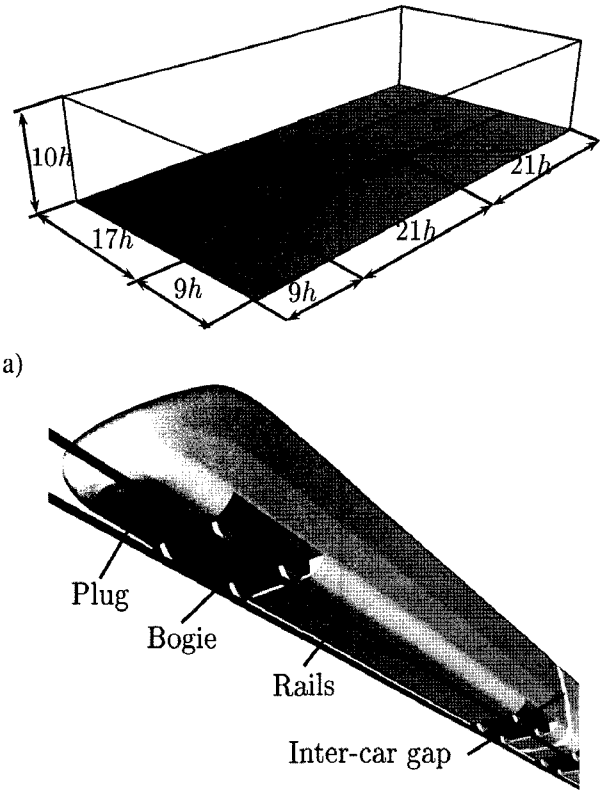

Fig. 2. a) Geometry of the Computational Domain of the High-speed Train Leaving the Tunnel. Here, h is the Height of the Train. b) Part of the Geometry of the Train Showing the Locomotive from Below

the wind gust condition is applied on both lateral walls and the inlet of the domain. This is done by changing the slip lateral boundary condition and the inlet constant streamwise velocity to the gust boundary conditions (described below). The resulting wind-gust boundary condition is a function in space that is changing in time. Thus the motion of the train out of the tunnel was simulated by changing the boundary conditions rather than moving the train in respect to the tunnel. Tunnels have smaller cross section than the computational domain used here and the possible limitation of the present approach could be that gusty conditions are changed ones they reach the position of the train. However, as we shall see later in the paper and in Fig. 1, this was not the case in the present work.

The mathematical model of the wind gust consists of a damping function, a saturation function and a sinusoidal function. These functions are then combined in the expression $V(t)=G_1+G_2+G_3$ where $G_1=B_1te^{-B_2t}$, $G_2=B_3erf(B_4t)$ and $G_3=1.5e^{B_5t}\sin(\Omega t)$. The values of the constants B_1-B_5 and Ω chosen in the present paper are presented in Table 1. Figure 1 shows the resulting gust model profile. As seen in this figure there is small difference between the profile at the boundary of the computational domain and the one at the position where the gust hits the train. This was achieved in the simulation by applying the identical boundary wind-gust condition (with opposite signs) on both lateral sides of the domain and using relatively small numerical time step. By doing so, we have made it possible for the wind gust to pass the domain virtually undisturbed except for the near wall (upper and lower walls) friction effects and blockage effects of the train and the rail. The resulting wind gust that reaches the train forms a maximal yaw angle of 36° with the direction of the train. The width of the wind gust is equal with the length of the train and the maximum velocity of approximately 40 [m/s] is at the position of 0.07 L (L is the length of the train) from the exit of the tunnel. The floor and the ceilings of the wind tunnel and the rail have the velocity equal to that of the air at the inlet. The lateral walls are treated as slip boundaries when the wind gust condition is not applied and no-slip boundary conditions are applied on the surface of the train. The outlet boundary condition is homogeneous Neumann. The wheels of the train are rotating and this has been achieved by putting the magnitude of the peripheral velocity of wheels equal to that of the rail, i.e. the inlet velocity.

The train used in the present paper is a model of an ICE2 high-speed train consisting of two locomotives and one car in the middle. The resulting total length of the model is approximately 79.5 [m]. The geometry of the front part of the train is shown in Fig. 2b and it includes

Table 1. Constants in the Mathematical Model of the Wind Gust

Constant	B_1	B_2	B_3	B_4	B_5	Ω
Value	750	9.5	15	150	4	200

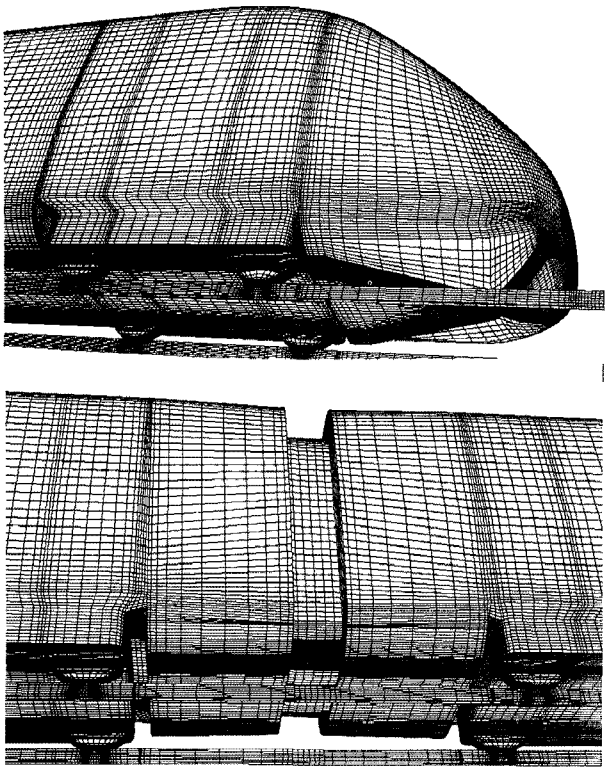

FIg. 3. Imprints of the Hexahedral Computational Grid on the Surface of the Train and the Rail. Rear Part of the Train (Upper Figure). Inter-car Gap between the Middle Car and the Rear Locomotive (Lower Figure)

bogies, rotating wheels, plugs and inter-car gaps. Besides, the rails were modelled in the simulation.

3. DES and Numerical Details

Detached Eddy Simulation (DES) with standard Spalart Allmaras (SA) model implemented in the commercial CFD solver Fluent 6.2 is used in the present paper. In a DES the distance from the wall in the SA model is replaced by the length scale that is the lesser of the distance to the nearest solid wall and a length proportional to the nearest grid spacing, i.e. $d=\min(d, C_{DES}\Delta)$ where $\Delta=\max(\Delta x, \Delta y, \Delta z)$. The constant C_{DES} is set to 0.65 in the present paper. The momentum equations have been discretized using second-order bounded scheme. The first order upwind scheme was used in the transport equation for the turbulent viscosity in the Spalart-Allmaras model. The time discretization of the equations was done using the second-order Crank-Nicolson scheme. The time step in

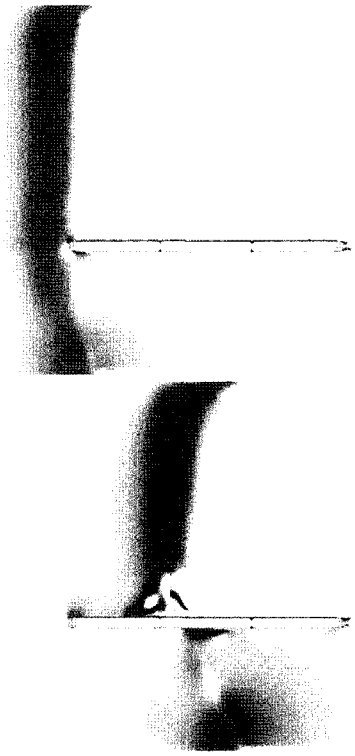

Fig. 4. Velocity Magnitude at the Mid Height of the Train at Two Times Where Gust Reaches the Train (Upper Figure) and the Gust is Approximately at the Middle of the Train (Lower Figure)

the simulation was $\Delta t=0.0005$ [sec] which produced the CFL number based on the height of the train h smaller than 1 in more than 99% off computational cells.

A structured hexahedral computational grid (Fig. 3) was made using commercial ICEM-CFD package. Multiple O-, C- and H- grid topologies were used in the construction of the grid. This meshing approach made it possible to obtain the necessary spatial resolution with a total of 15.5 million computational cells.

4. Results

In the present paper we concentrate on understanding of the flow mechanisms when the train travels through a wind gust. Figure 4 shows the resulting propagation of the wind-gust model through the domain. As seen here, the gust propagates relatively undisturbed between the two lateral sides of the domain. This together with the resulting profile from Fig. 1 shows that the desired flow conditions were achieved.

Figure 5 shows the development of the flow structures on the leeward side of the train as the train travels through the wind gust. Immediately after the train starts to exits the tunnel, several trailing vortices are formed on the leeward side of the train of which the strongest one, T_M, origins at

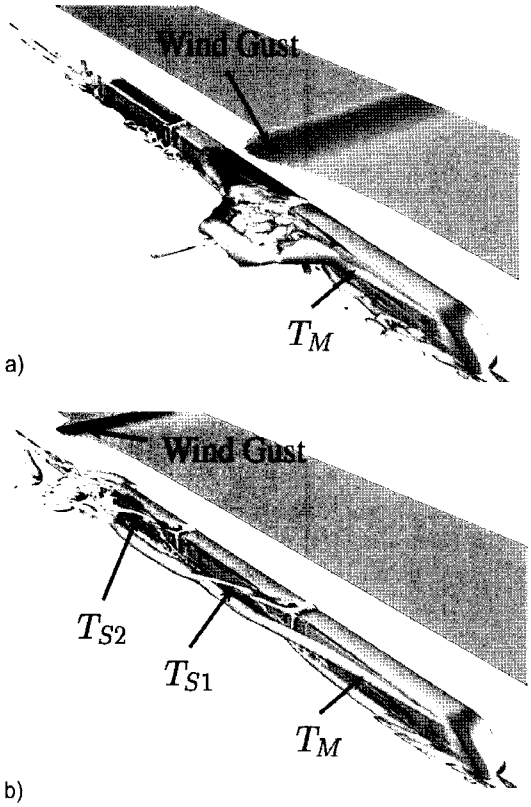

Fig. 5. An Isosurface of the Second Invariant of the Velocity Gradient Coloured with Velocity Magnitude at Two Times Corresponding to a) $x/L=0.63$ and b) $x/L=1.58$

approximate position of the upper front corner of the train. As the train passes the gust region and enters the steady cross wind, the T_M vortex becomes the dominant structure in the flow (Fig. 5b). However, as the inter-car gaps enter the wind gust, secondary trailing vortices, T_{S1} and T_{S2}, are formed (Fig. 5b). These two vortices enter the main trailing vortex T_M after some short length of free formation.

Pressure contributions to all aerodynamic force and moment coefficients were computed and presented in Figs. 6 and 7 as functions of position of the front of the train from the tunnel exit. Note that friction forces were not taken into account in the present paper. When computing the force and moment coefficients the reference length and cross sectional area of the train are chosen as $l=3$ [m] and $A=10$ [m^2], respectively, following the practice in train aerodynamics. All three moments were computed around the origin located in the middle of train's length and in the plain of contact of wheels with the track (see Fig. 2a).

The drag, the side and the lift forces are forces acting in the x, y and z directions, respectively. Similarly, the rolling, pitching and yawing moments are those acting around the x, y and z axes. First observation from Figs. 6 and 7 is that the drag, C_D, and the side force, C_S, as well as the moments resulting from C_S, i.e. the rolling, C_{RM}, and the

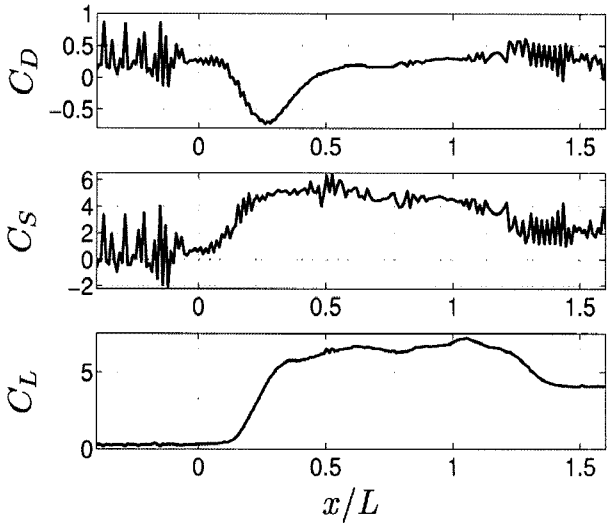

Fig. 6. Aerodynamic Force Coefficients (Pressure Part) as a Function of the Position of the Front of the Train from the Tunnel Exit

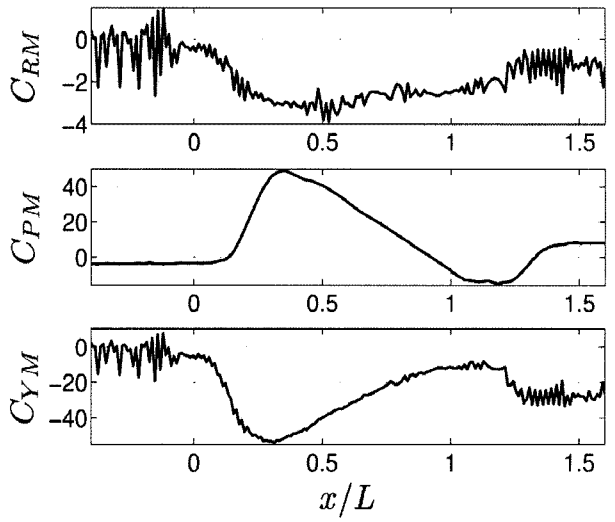

Fig. 7. Aerodynamic Moments Coefficient (Pressure Part) as a Function of the Position of the Front of the Train from the Tunnel Exit

yawing, C_{YM}, moments are more unsteady in regions outside the gust's influence. Another interesting observation is that of negative pressure drag which reaches its minimum of $C_D=-0.73$ ones one fourth of the train has left the tunnel. This is due to the strong under pressure on the front of the train caused by the cross flow (see Fig. 8).

It was also found that the maximal lift force is obtained some time after the entire train has left the tunnel. The exact position of maximal $C_L=7.22$ is when the tail of the train is only 0.018 L from the maximum wind-gust velocity position.

The explanation for the strong lift force at this time position is given in Fig. 9. The resulting flow produces the

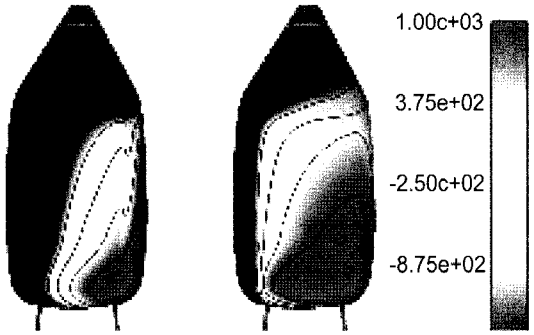

Fig. 8. Surface Pressure on the Train at Two Times Corresponding to: $x/L=0.25$ (left) and $x/L=1.3$ (Right). View of the Front of the Train

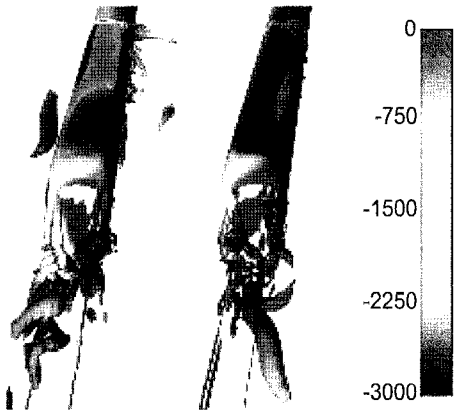

Fig. 9. Surface Pressure on the Train at Two Times Corresponding to: $x/L=1.054$ (left) and $x/L=1.6$ (Right). View of the Rear of the Train

static pressure on the upper side of the rear locomotive which is much lower from that after the train has left the wind gust. The side force and the resulting rolling moment reach their maximum and minimum, respectively, of $C_S=6.4$ and $C_{RM}=-3.9$ when the front of the train has position $x/L=0.53$ after the exit of the tunnel. Figure 10 shows the flow structures and the resulting pressure on the surface of the front locomotive at the position of maximal negative rolling moment. The main trailing vortex is very strong at this position causing large regions of low pressure close to the upper edge of the leeward side of the train. The difference in the flow structures and the resulting surface pressure between the position of maximal negative rolling moment and the position when the train is in constant crosswind is presented in Fig. 11. Obviously gusty wind conditions produce stronger trailing vortex on the leeward side of the train resulting in lower pressure on the leeward side of the train.

When comparing the aerodynamic force coefficients for the train inside the tunnel and in the constant crosswind of 15 [*m/s*] (i.e. when the train has passed through the wind-

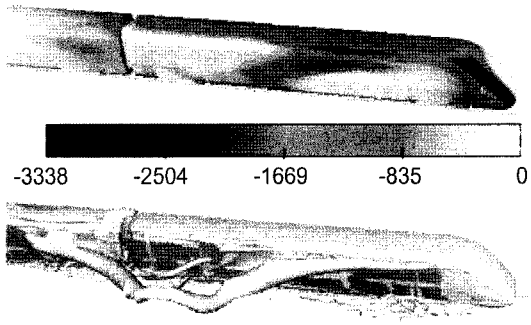

Fig. 10. a) Surface Pressure on the Train and b) Flow Structures at the Time Corresponding to $x/L=0.53$

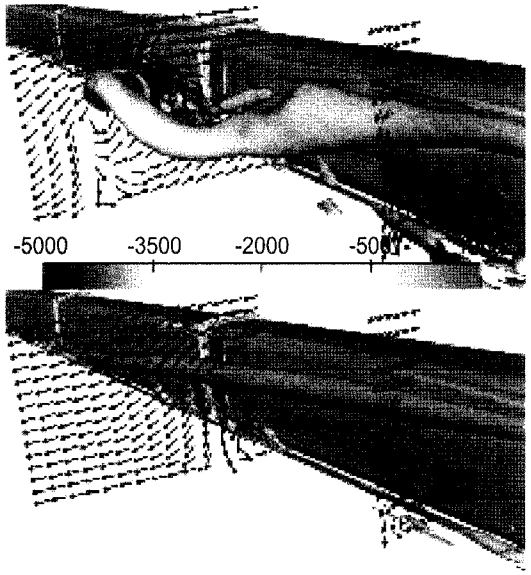

Fig. 11. Flow Structures Behind the Leeward Side of the Train at Position Corresponding to $x/L=0.53$ (Upper Figure) and $x/L=1.6$ (Lower Figure). View is of the Front Locomotive and Flow is from Right to Left. Body of the Train is Coloured with Static Pressure. Note that the Velocity Vectors are for Clarity Reasons Uniformly Distributed in the Figure and that Actual Computational Grid is Much Finer

gust region), we find that the C_D increases only marginally from 0.25 to 0.3 while the increase in C_S and C_L is mach larger, from 1.25 to 2 and from 0.27 to 4.1, respectively.

Another observation is that the influence of the wind gust on the aerodynamic forces stops at time corresponding to approximately $x/L=1.45$, i.e. when the entire train has left the most of the width of the wind-gust region. Thus, it seems that there are no history effects of the wind gust on the aerodynamic forces. Similar is valid for the aerodynamic moments (Fig. 7).

The minimum yawing and maximum pitching moments were observed at times corresponding to $x/L=0.32$ and $x/L=0.35$, respectively. Figure 12 shows that at this position the main trailing vortex is concentrated close to the upper

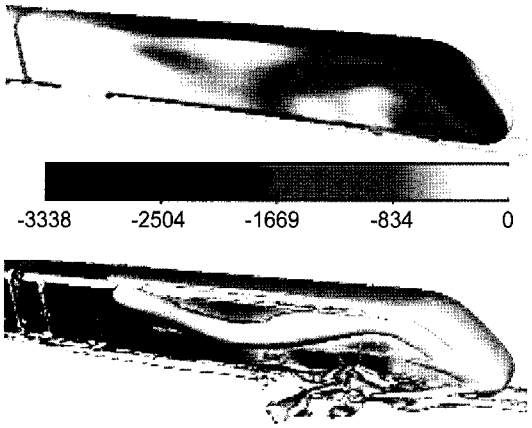

Fig. 12. a) Surface Pressure on the Train and b) Flow Structures at the Time Corresponding to $x/L=0.35$

front corner on the leeward side of the train resulting in a region of low pressure in a confined area of the front upper corner. The resulting effect of this vortex is similar to that of a lever attached to the location of the low pressure region on the train.

The pitching moment changes its sign from negative to positive at approximately $x/L=0.14$ to return to negative at $x/L=0.92$. The final change to positive pitching moment occurs at $x/L=1.33$ with the result that the front of the train wants to lift in the constant crosswind.

Formation of the recirculation region on the windward side of the train and close to the ground shown in Fig. 13 was observed as the train passes wind gust but also directly after its passage. This structure is a direct result of the strong crosswind velocity in this region and small ground clearance of the train.

5. Conclusions and Discussion

The present paper presents a numerical study of a wind-gust scenario where the flow conditions are changing from those when the train is shielded by an obstacle (tunnel), over those where the crosswind profile is varying to a flow region with constant crosswind. This is similar to real conditions where the wind gust is limited in space [5]. However, there are other scenarios that are interesting such as train travelling on an embankment or a bridge and influenced by a wind gust during some limited time. In these two scenarios (in particular in the later one) the crosswind velocity is higher than in the present scenario due to relatively small boundary layer effects on the height of the bridge or acceleration of the flow in the case of the embankment. In the present paper we have used relatively large maximal wind-gust velocity of 40 [*m/s*].

Although such crosswind velocity is probably too large for a real gusty conditions it helps to study the worst possible scenario e.g. when a train exits a tunnel on a high bridge under the influence of a wind gust. An example of such a situation in Sweden is the train that exits the tunnel on the resunds bridge between Sweden and Denmark. An additional gain of using this high crosswind velocity is that the computational effort can be decreased. The reason for this is that the larger crosswind velocity - the longer length propagates the effect of the lateral boundary conditions for a fixed numerical time step. Thus the proper implementation of an undisturbed crosswind front throughout the lateral direction of the domain is directly dependent on the crosswind velocity and the numerical time step.

The present study used only one shape of wind gust and performing simulations with other crosswind velocities and widths of gusts are needed for drawing general conclusions. Although the present wind-gust scenario is very close to the reality is was in the past assumed complex and difficult to implement in simulations [5]. However, with the present approach it is expected that the parametric studies will become affordable in the near future. Ones the flow with the train in the tunnel has developed in the simulation, several wind-gust simulations (with different velocity magnitudes and widths of the gust) can be run in parallel. For a comparison we can mention that the present simulation used 40 processors (Xeon 5160 with 3 GHz cores) during 2 weeks for the flow developments in the tunnel and additional one week for the simulation of the wind-gust passage. This is today considered computationally expensive but the computational effort is expected to decrease with the development of the computer hardware.

The present work has for the first time given an insight into the course of events of a high-speed train passing a realistic wind-gust. Using a powerful time-dependent numerical simulation technique we were able not only to follow the history of the resulting aerodynamic forces and

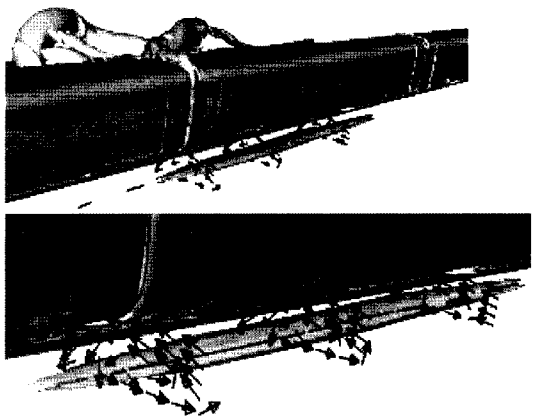

Fig. 13. Flow Structure on the Windward Side of the Train at $x/L=0.5$ (Upper Figure). Zoom of the Structure with its Vortex Core (Lower Figure)

moments acting on the train but also to explain the underlying flow mechanisms. Although relatively detailed representation of the train was used in our simulation, effects of motion of vehicles except along the track were not considered here. Besides, the inclination of vehicle in curves is not considered. The later assumption is probably more serious constrain of the present simulation as the high-speed trains used in Sweden are tilting trains. The direct consequence of the inclination of the train in a strong curve is that resulting flow around the train becomes very different from that when the train is travelling on a straight track. However, the use of the zero inclination of the train in the present paper is justified by the scenario of a tunnel exit and relatively short wind-gust width which minimize the aerodynamic effect of possible inclination of the train.

The important consequence of the present approach is that we have been able to relate the aerodynamic behaviour of a train in gusty conditions to the flow structures and their interaction with the train. These are directly dependent on the train design and combination of the present prediction technique with optimization techniques such as that described by Krajnović [6] makes it possible to design high-speed trains with optimal crosswind stability properties.

Acknowledgments

This work is financed by Banverket (Swedish National Rail Administration) under the contract no. HK 06-1337/AL50 and it is a part of the programme called Gröna Tåget (eng. Green Train). ANSYS Sweden and Bombardier Transportation are supporting the project. Computer time at SNIC (Swedish National Infrastructure for Computing) resources at the centre for scientific and technical computing at Chalmers (C3SE) is gratefully acknowledged.

Reference

1. Howell, J. P. and Everitt, K. W., 1983, Gust response of a high speed train model. In Aerodynamics of Transportations II (eds T. Morel & J. Miller), pp. 81-89, New York: ASME
2. Howell, J. P., 1986, Aerodynamic response of maglev train models to a crosswind gust, Journal of Wind Engineering and Industrial Aerodynamics, 22 205-213.
3. Kobayashi, N. and Yamada, M., 1988, Stability of a One Box Type Vehicle in a Cross-Wind-An Analysis of Transient Aerodynamic Forces and Moments, SAE paper No. 881878.
4. Ryan, A. and Dominy, R. G, 2000, Wake Survey Behind a Passenger Car Subjected to a Transient Cross-Wind Gust, SAE paper No, 2000-01-0874
5. Carrarini, A., 2006, Reliability based analysis of the crosswind stability of railway vehicles, Dissertation Thesis, TU Berlin.
6. Krajnovi, S., 2007, Optimization of the aerodynamic properties of high-speed trains with CFD and response surface models, In Proceedings of The Aerodynamics of Heavy Vehicles II: Trucks, Buses and Trains, Tahoe City, USA, August 26-31.